Journal of Applied Polymer Science

Intumescent Flame Retardant Polyurethane/Starch Composites: Thermal, Mechanical, and Rheological Properties

Jaber Nasrollah Gavgani,[1,2] Hossein Adelnia,[1] Gity Mir Mohamad Sadeghi,[1] Farhad Zafari[1]

[1]Department of Polymer Engineering and Color Technology, Amirkabir University of Technology, Tehran, Iran

[2]Department of Chemical Engineering, Amirkabir University of Technology, Tehran, Iran

Correspondence to: Gity Mir Mohamad Sadeghi (E-mail: gsadeghi@aut.ac.ir)

ABSTRACT: Intumescent flame retardant polyurethane/starch (IFRPU/starch) composites were prepared by means of melt blending. Microencapsulated ammonium polyphosphate (MCAPP) was added to improve its compatibility with matrix, retardation of reaction between acid and carbon source, and its water resistancy. Fourier transform infrared spectroscopy (FTIR) confirmed the presence of hydrogen bonding and entangled network between IFR system and PU matrix. Further, scanning electron microscopy (SEM) illustrated homogeneity of starch in matrix. By addition of 10 wt % of starch and 20 wt % of IFR, limiting oxygen index (LOI) increased from 22.0 to 40.0 and UL94 V0 rating was achieved. Differential scanning calorimetry (DSC) detected three endothermic transitions and one glass transition (T_g). The temperature of transition III and T_g increased with starch due to crosslinking between PU and starch. The improved thermal stability in the presence of starch was confirmed by thermogravimetric analysis (TGA). Beside the fact that starch was used as a carbonization agent to improve flame retardancy, it also effectively led to enhanced mechanical and viscoelastic properties. © 2014 Wiley Periodicals, Inc. J. Appl. Polym. Sci. **2014**, *131*, 41158.

KEYWORDS: composites; polyurethanes; properties and characterization; rheology; thermal properties

Received 3 March 2014; accepted 12 June 2014

DOI: 10.1002/app.41158

INTRODUCTION

The improvement of the thermal stability and fire resistance properties of polyurethane (PU) are major concerns, particularly in the domains of transportation, building, coatings, leather, automatic applications, etc.[1–3] This is usually carried out by the addition of flame retardant additives into the polymer. Currently, it is possible to treat most potentially flammable materials with special additives to make them more difficult to ignite and to significantly reduce the fire spread. Therefore, researchers have started extensive investigation to achieve high performance PU with high oxidative stability and flame retardancy.[4]

Depending on their nature, flame retardant systems can act either physically (by cooling, forming a protective layer, or by diluting the fuel) or chemically through a reaction in condensed or gas phase. They can interfere with the different processes involved in polymer combustion such as heating, pyrolysis, ignition, and propagation of thermal degradation. The most common flame retardant systems contain halogens, phosphorus, inorganic, and nitrogen containing compounds.[5] Recently, some halogen flame retardant compounds have been demonstrated as being environmentally unfriendly due to production of much smoke and toxic gases during burning.[6]

Intumescent flame retardants (IFR) are considered as thriving halogen-free flame retardant additives. Besides the fact that aforementioned problems associated with halogen containing can be eliminated by employing IFR, they can also result in lower corrosion and preventing molten dropping during fire.[7–10] The most important characteristics of IFR containing composites are their ability to swell and to foam under heat radiation.[11] To severely reduce oxygen access to the substrate and to extremely reduce fuel transport into the flame, the main constituents of intumescent systems should consist of an acid source, a swelling agent, and a carbon source, which are also called dehydrating agent, spumific, and carbonific, respectively.[12,13]

An acid source such as ammonium polyphosphate (APP) reduces the fuel feeding to the flame, first by catalyzing the formation of anhydride intermolecular bridges (reticulation) and then by stopping the intramolecular degradation. These reactions result in cyclizations, playing role of precursor of charring phenomena and allowing the formation of a physical barrier over the surface of material.[14] APP is widely used in the form of microencapsulated to improve its interfacial adhesion with matrix,[15] retardation of reaction between acid and carbon source,[16] and enhancement of its water resistancy.[17] A swelling agent, such as melamine (MA), facilitates the formation of an

Table I. Formulations of Pure PU and IFRPU/Starch Systems (by Mass Percentage)

Samples	PU	IFR[a]	Starch
Pure PU	100	0	0
PU-0	80	20	0
PU-2.5	70	27.5	2.5
PU-5	70	25	5
PU-10	70	20	10

[a] IFR contains MCAPP/MA blend at a mass ratio of 2/1.

expanded barrier layer by releasing an inert gas (NH_3, CO_2, and H_2O).[18] A carbon source such as starch produces a cross-linked char layer which causes self-extinguishing phenomena by preventing oxygen feeding to the flame. Starch is an abundant, inexpensive, biodegradable, biocompatible, and renewable polyhydric polyol,[19] which could be used as a natural carbon source. It has been incorporated into various polymers, such as polyethylene, poly(lactic acid), polycaprolactone, etc to meet the vital requirements for various applications.[20–24]

Incorporation of fillers will generally improve viscoelasticity and flame retardancy, which is usually accompanied by a liquid-like ($G' \sim \omega^2$) to solid-like ($G' \sim \omega$) transition in the terminal or low frequency as fillers loading reaches the percolation threshold value.[25,26] From another point of view, mechanical, viscoelasticity, and flame retardancy properties typically represent the performances of polymer composites at three stages, including operation, processing, and combustion temperature, respectively.

To the best of our knowledge, few studies have examined the combination of starch with IFR as a flame retardant system. In this study, a novel IFR mixture composed of MA, microencapsulated ammonium polyphosphate (MCAPP) with starch was blended with PU to obtain flame retardant and environment friendly composites. Finally, the thermal stability, flame retardancy, rheological, and mechanical properties as well as their quantitative relationship have been investigated.

EXPERIMENTAL

Materials

Thermoplastic PU (Desmopan 5377 A) was purchased from Bayer Co. (Germany). MCAPP (average size 10 μm) by PU was provided from Hefei Keyan Co. (China). MA was supplied from Sigma Aldrich Co. The IFR was composed of MCAPP and MA (the mass ratio was 2 : 1). Potato starch was supplied from Fluka Co.

Preparation of Samples

PU, MCAPP, MA, and starch were dried in a vacuum oven at 80°C for 24 h before melt processing. PU pellets were fed to the twin screw extruder at a rate speed of 60 rpm at 140°C. The IFR was then poured and mixed at the same speed for 2 min. Starch was gradually added into the extruder, while blending. The mixture was blended at 60 rpm for 15 min and was allowed to cool at room temperature. After mixing, the samples were hot-pressed at about 140°C under 10 MPa for 10 min into sheets with the thickness of 3.0 ± 0.1 mm for UL-94 and limiting oxygen index (LOI) test, whereas 2.0 ± 0.1 mm for DIN 4102 standard test. The formulations of prepared samples are presented in Table I.

Differential Scanning Calorimetry (DSC)

The transition behavior of the intumescent flame retardant polyurethane (IFRPU)/starch composites was characterized using DSC (Mettler TC 10A/TC 15, TA controller). The samples were heated from 25 to 600°C using an aluminum crucible with perforated cover and ~5.0 mg of each sample, under a synthetic N_2 flow of 150 mL min^{-1} at a heating rate of 10°C min^{-1}.

Thermogravimetric Analysis (TGA)

TGA was carried out using a Q5000IR (TA Instruments) thermoanalyzer instrument at a linear heating rate of 10°C/min under a Nitrogen flow. Samples have been tested in an alumina crucible with a mass of about 5.0 mg. The temperature reproducibility of the instrument was ±1°C, whereas the mass reproducibility was ±0.2%.

The theoretical TGA curve was computed by linear combination between the TGA curves of pure PU, IFR, and starch. The formula is as follows[27]:

$$W_{th}(T)_{IFRPU/starch} = x \times W_{exp}(T)_{PU} + y \times W_{exp}(T)_{IFR} + z \times W_{exp}(T)_{starch}, x + y + z = 1$$

where $W_{th}(T)_{IFRPU/starch}$: theoretical TGA curve of the IFRPU/starch composites; $W_{exp}(T)_{PU}$: experimental TGA curve of the pure PU; $W_{exp}(T)_{IFR}$: experimental TGA curve of IFR; $W_{exp}(T)_{starch}$: experimental TGA curve of starch; x, y, and z are the mass percentages of the PU, IFR, and starch in the composites, respectively.

Table II. The Flame Retardancy of Pure PU and IFRPU/Starch Composites (with Standard Deviations in Parentheses)

Sample	LOI (%)	UL-94 rating	Time of burning (sec)
Pure PU	22.0 (0.60)	Burning	40 (0.35)
PU-0	29.0 (0.55)	V1	75 (0.43)
PU-2.5	33 (0.40)	V0	Self-extinguished
PU-5	35 (0.40)	V0	Self-extinguished
PU-10	40 (0.41)	V0	Self-extinguished

Limiting Oxygen Index (LOI) and UL-94 Tests

LOI was measured with an HC-2 oxygen index meter (Dynisco, USA). The dimensions of used specimens for the LOI test were 100 × 6.5 × 3 mm^3. The vertical test was carried out on a UL-94 chamber (Concept Fire Testing, UK) according to the UL-94

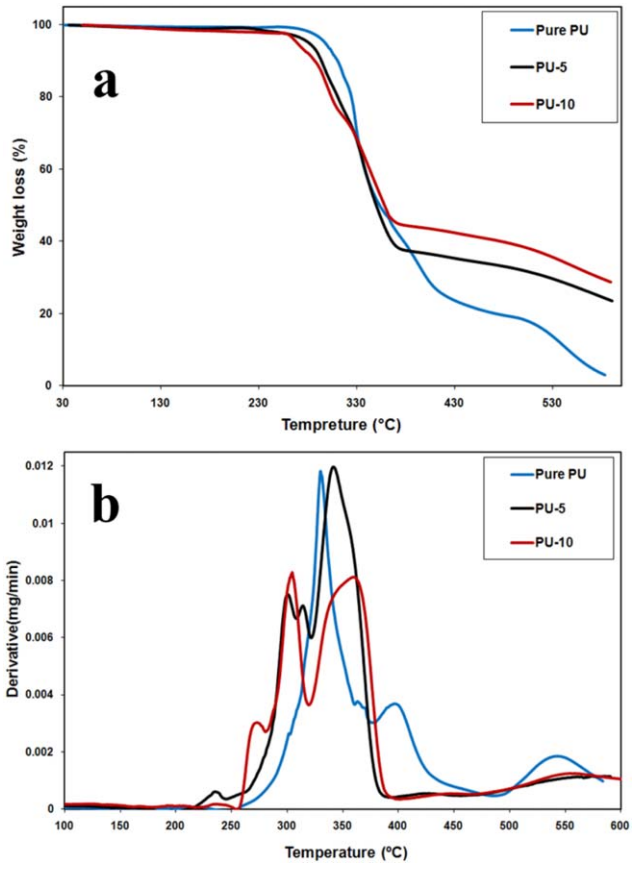

Figure 1. (a) TGA and (b) DTGA traces for pure PU and IFRPU/starch composites in nitrogen atmosphere. [Color figure can be viewed in the online issue, which is available at wileyonlinelibrary.com.]

test standard. The dimensions of used specimens for the UL-94 test were 130 × 13 × 3 mm^3. To measure burning times of various samples, 40 × 10 × 2 mm^3 bars were prepared and burning time to 2 cm-mark lines was measured according to Clause 6.2.5 of DIN 4102 standard. It should be added that LOI is defined according to ASTM D2863 in which the specimen is placed vertically in a test column and a mixture of oxygen and nitrogen is passed over the column. Then, the specimen is ignited at the top. The concentration of oxygen is reduced until the specimen just supports combustion. The concentration is reported the volume percent. The results of UL-94 tests represent after flame and afterglow time in seconds for a specimen with specified shape. The results are defined in three distinct categories as follow: (i) V-0: burning stops within 10 sec on a vertical specimen; no flaming drips are allowed. (ii) V-1: burning stops within 30 sec on a vertical specimen; no flaming drips are allowed. (iii) V-2 burning stops within 30 sec on a vertical specimen; drips of flaming particles are allowed.

Table III. TGA Data of Pure PU and IFRPU/Starch Composites Under Nitrogen Atmosphere

Samples	$T_{d,5\%}$ (°C)	$T_{d,70\%}$ (°C)	T_{max} (°C)	Char residue (%) at 600°C
Pure PU	297	407	328	3
PU-5	281	526	300, 308, 334	24.7
PU-10	275	578	267, 300, 344	29.3

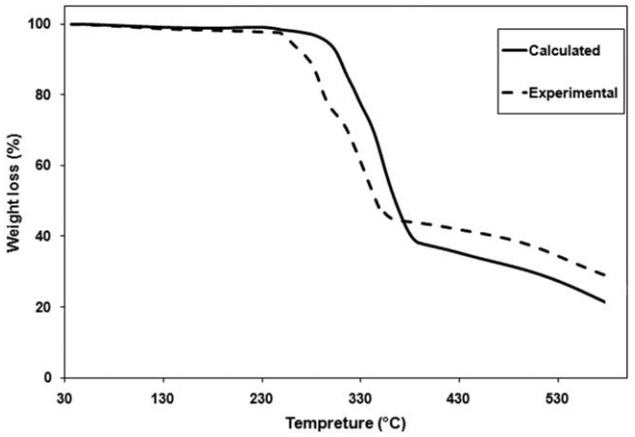

Figure 2. Mass loss difference between the experimental and theoretical TGA curves for PU-10.

Fourier Transform Infrared Spectroscopy (FTIR)

FTIR spectra of the samples were obtained using Equinox 25 Bruker (Canada). Typically, 1–2 mg samples were mixed with 100 mg of potassium bromide powder and pressed into pellets. All the spectra are the average of 32 scans taken in the wave number range of 4000 to 400 cm^{-1}.

Scanning Electron Microscopy (SEM)

SEM was performed on the fractured surfaces of samples and cross sections of the char residues using a Philips Xl30E at acceleration voltage of 20 kV. The specimens were previously coated with a conductive layer of gold.

Mechanical Properties

Mechanical properties of the samples were tested with a Galdabini Sun-2500 Universal Testing machine according to ASTM D 683. At least three samples were tested to obtain mean values as well as standard deviations.

Rheological Properties

Rheological properties were evaluated using an ARES (Anton Paar, Germany) with parallel plate geometry of 25 mm in diameter at 140°C. The linear viscoelastic region was determined by monitoring storage modulus in dynamic strain amplitude sweep experiment. Dynamic frequency sweeping tests were measured with the frequency (ω) from 0.01 to 1000 rad sec^{-1}.

RESULTS AND DISCUSSION

Flame Retardancy of Pure PU and IFRPU/Starch Composites

The synergistic effect of starch on the LOI values and UL-94 results of the IFRPU/starch composites are shown in Table II. Although flame retardancy is greatly improved by incorporation of MCAPP and MA, it is not still classified in UL-94 V0 rating. Moreover, it can be seen that the LOI values of the IFRPU/starch composites increase with starch increment. By incorporation of IFR with starch, both PU-5 and PU-10 can pass the V0

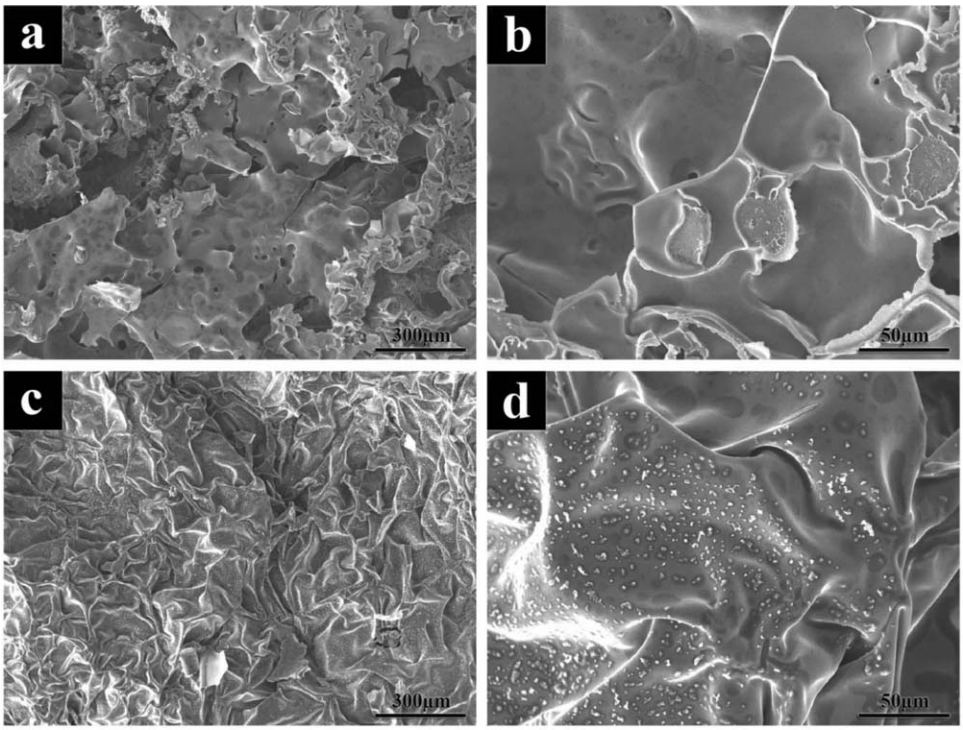

Figure 3. SEM micrograph of PU-5 and PU-10 char residue obtained from LOI test: (a) PU-5, ×150, (b) PU-5, ×900, (c) PU-10, ×150; (d) PU-10, ×900.

rating in the UL-94 test, while the PU-0 reaches V1 rating. The results of DIN 4102 standard confirm LOI values too. Ni et al.[28] reached UL-94 V0 rating in the presence of 30 wt % MCAPP, whereas Duquesne et al.[29] achieved the LOI value of 44 by addition of 40 wt % APP. In comparison with the findings of aforementioned studies, one can realize that this IFR mixture with starch effectively improve flame retardancy of PU in contrast with MCAPP alone. Thus, it can be concluded that starch is an efficient carbonization agent for PU, which not only promotes the formation of the protective char layer (will be discussed in section "Char morphology of IFRPU/starch composites"), but also contributes to self-extinguishing phenomenon.

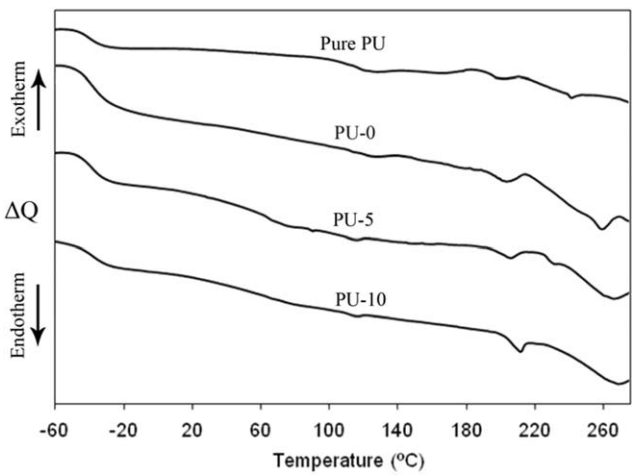

Figure 4. DSC curves of pure PU and IFRPU/starch composites.

Thermal Stability of Pure PU and IFRPU/Starch Composites

The typical TGA and DTGA traces for pure PU and IFRPU/starch composites under nitrogen atmosphere are given in Figure 1(a,b), respectively. The initial decomposition temperature ($T_{d,5\%}$) can be considered as the temperature at which the mass loss is 5%. The relative thermal stability of the samples was compared by mean of the temperature of 5% ($T_{d,5\%}$), 70% ($T_{d,70\%}$) mass loss, the temperature of maximum rate of mass loss (T_{max}), and the percent char yield at 600°C. These data are listed in Table III.

Pure PU had a two-step degradation process at 250–380, 380–420°C. The former is ascribed to the dimerization and trimerization reaction of isocyanates,[30,31] whereas the latter is mainly attributed to depolymerization of PU to form isocyanate, polyol, primary or secondary amine, olefin, and carbon dioxide.[32]

As for IFRPU/starch systems, the thermal degradation of PU-5 and PU-10 has three stages at 250–280, 280–315, and 315–380°C. The first stage is assigned to the degradation of MA,[33,34] whereas the second one is due to starch hydroxylation and decomposition of MCAPP.[22,35] The last stage is also ascribed to depolymerization of PU.[32,36] Besides, the second degradation step in pure PU has disappeared in the presence of IFR system.

The $T_{d,5\%}$ of IFRPU/starch composites are around 240–300°C, which are lower than that of pure PU. The decrease of $T_{d,5\%}$

Table IV. Glass Transition, Melting Point, Heat of Fusion, and Total Heat of Fusion of Pure PU and IFRPU/Starch Composites (with Standard Deviations in Parentheses)

		T_m (°C)			ΔH_f (J/g)			
Samples	T_g (°C)	I	II	III	I	II	III	$\Delta H_{f,\ Total}$ (J/g)
Pure PU	−40.05	120.07	197.70	243.07	8.98	0.86	2.41	12.25 (0.40)
PU-0	−37.83	126.54	201.85	259.21	8.42	1.21	6.36	15.99 (0.45)
PU-5	−34.96	124.26	209.56	264.37	8.26	1.86	8.56	18.68 (0.36)
PU-10	−32.26	122.93	213.12	269.87	8.78	2.26	10.48	21.52 (0.34)

and thermal stability is due to the breakage of weak P—C bond of MA and formation of polyphosphoric acid, accelerating the decomposition of IFRPU systems as a strong Lewis acid catalyst.[37] On the other hand, the T_{max}s of IFRPU/starch composites are higher than that of pure PU, indicating that incorporation of starch has effectively improved thermal stability of the composites. In fact, this improved thermal stability is due to the high grafted crosslinking of the PU with starch[38] and hydrogen bonding between carbonyl of PU and hydroxyl of starch[39] (will be discussed later). The $T_{d,70\%}$ was enhanced by the addition of starch which reflects the thermal stability of the char layer formed during degradation. More importantly, as starch was combined with IFR, the residue left at 600°C increased significantly. Moreover, at higher temperatures (beyond 500°C), the mass loss kinetic is lower than that of pure PU. APP can form phosphoric anhydrides or the related acids at higher decomposition temperature which consequently promote the char formation.[27] These phosphor-carbonaceous chars are more stable than carbonaceous alone obtained from pure PU. These observations along with the results of LOI and UL-94 tests indicate that the incorporation of the starch into IFRPU systems notably improves the thermal stability of the composites and further enhances char formation. In fact, flame retardant behavior of starch is primarily due to its capability to form a continuous, protective char layer that acts as a thermal insulator and a mass transport barrier.[40,41]

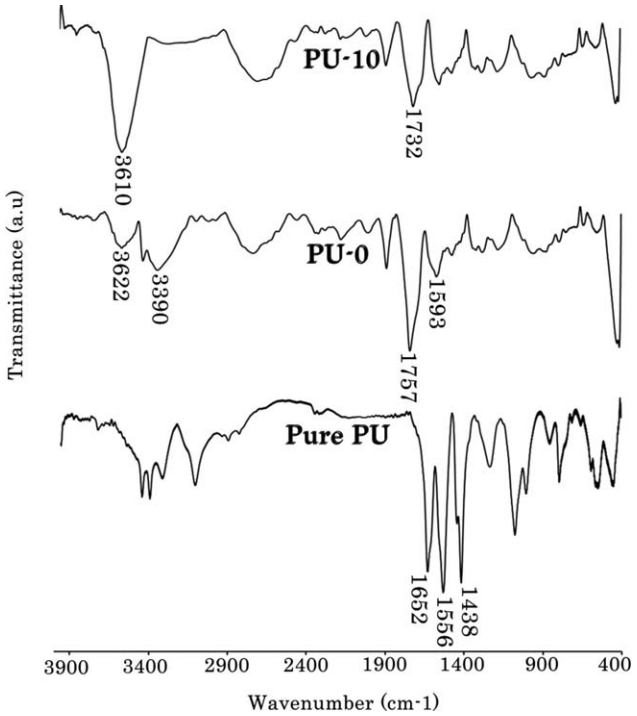

Figure 5. FTIR spectra of pure PU and IFRPU/starch composites.

In analogy with what has recently been done by Wang et al.,[27] the theoretical TGA curve of PU-10 was calculated and compared with actual TGA curve (Figure 2). It can be seen that the actual residue (29.3%) of PU-10 at 600°C is higher than the calculated one (17.8%). As compared with the calculated curve, the experimental one exhibits higher thermal stability and char yield at higher temperature (>350°C). This indicates the presence of a synergism between IFR and starch on the char formation and flame retardancy.

Char Morphology of IFRPU/Starch Composites

The SEM micrographs of chars from the surfaces of PU-5 and PU-10 are shown in Figure 3. As it can be seen, surface morphology of PU-5 char is not homogenous and there are some flaws. Thus, volatile components can easily diffuse from the lower layer of char to the flame zone.[42] On the contrary, the PU-10 char surface morphology is so homogenous that a blanket-like structure is formed. This kind of structure considerably acts as a protective barrier layer; consequently, it restricts the oxygen diffusion to the surface.[43,44]

Table V. Mechanical Properties of Pure PU and IFRPU/Starch Composites

Sample	Tensile strength (MPa)	Elongation at break (%)	Modulus (MPa)
Pure PU	4.42 (0.18)	385.34 (2.36)	5.46 (0.22)
PU-0	4.11 (0.09)	345.87 (2.15)	6.23 (0.49)
PU-2.5	5.75 (0.42)	331.67 (2.38)	8.53 (0.56)
PU-5	6.85 (0.25)	324.34 (3.16)	13.12 (0.33)
PU-10	8.38 (0.18)	313.21 (2.61)	17.34 (0.30)

Mean values and standard deviation (in parentheses).

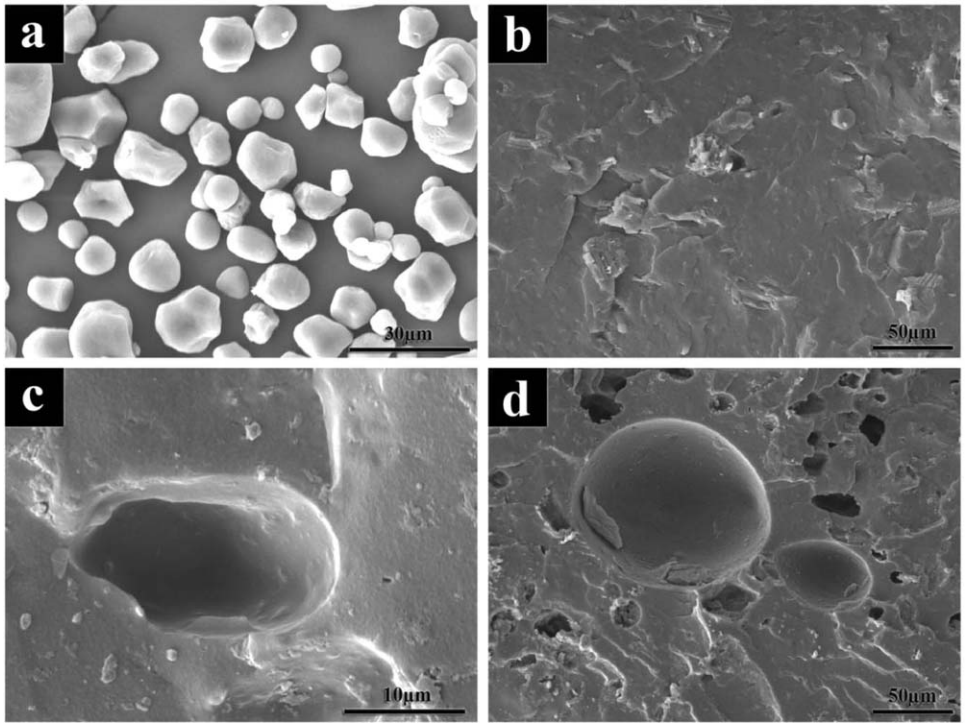

Figure 6. SEM micrographs of (a) neat starch, (b) unextracted fractured surface of PU-10, (c) starch extracted of PU-10 (×6000), and (d) ×800.

Thermal Transition of Pure PU and IFRPU/Starch Composites

Transitions of IFRPU/starch composites are shown in Figure 4 and Table IV. One glass transition (T_g) and three endothermic transition regions at 80–140°C (endothermic I), 160–220°C (endothermic II), and 240–270°C (endothermic III) are shown in Figure 4. All reported DSC glass transition temperatures are evaluated from the so-called "mid-points," i.e., the temperature at which the measured curve crosses the imaginary line that is drawn exactly between the two extrapolated baselines. T_g was increased by the addition of starch thanks to the interaction of PU chains with starch. These three endothermic peaks are assigned to various morphology of PU hard segment. Incorporation of IFR components and starch in PU leads to some variation in transitions region which is due to PU/MA and PU/starch crosslinking. It is noteworthy to point out that starch is a polyol which shows a crosslinked and complex network with PU. Transition I can be assigned to short-range hard segment morphology that has been shifted to the higher temperature with IFR incorporation.[45–47] On the contrary, it was decreased by starch increment. Transition II is attributed to dissociation of long range ordering in microphase hard segment which increases by starch.[47] Transition III is ascribed to the hard segment melting point which rises by starch. The reason for this is crosslinking between PU and starch which increases hard segment arrangement due to the stretching behavior of starch granules. Moreover, the total heat of fusion related to the transition I, II, and III increases by starch incorporation. This is in good agreement with mechanical properties shown in Table IV.

Chemical Characterization of Pure PU and IFRPU/Starch Composites

Figure 5 shows FTIR spectra of pure PU and IFRPU/starch composites. Since APP has been encapsulated by PU, elucidation of its interaction with other components would be neglected; thus, comparing the spectra of Pure PU with PU-0 reveals interaction between MA and PU, whereas the spectrum of PU-0 and PU-10 comparison clarifies the crosslinking of PU and starch.

When compared with the spectra of Pure PU, three sharp peaks (1652, 1556, and 1438 cm^{-1}) have disappeared, whereas two new peaks (1757 and 1593 cm^{-1}) have appeared in PU-0. This is attributed to the absorption of urethane linkages between MA component and PU.[48] On the other hand, as the starch was introduced into the composite, peaks of 3390 and 3622 cm^{-1} merged and sharp peak formed around 3610. Moreover, the shift of carbonyl peak around 1703–1732 cm^{-1} further verifies hydrogen bonding between PU and starch.[47]

Mechanical Properties of Pure PU and IFRPU/Starch Composites

Mechanical properties of Pure PU and IFRPU/starch composites are shown in Table V. As it can be seen, addition of 20.0 wt % IFR leads to a reduction in tensile strength. These additives at high loading have a detrimental effect on the mechanical properties of the polymer matrix.[49,50] On the other hand, as compared with the PU-0, tensile strength increased for IFRPU/starch composites. Good state of starch dispersion in matrix which is because of good interaction and crosslinking

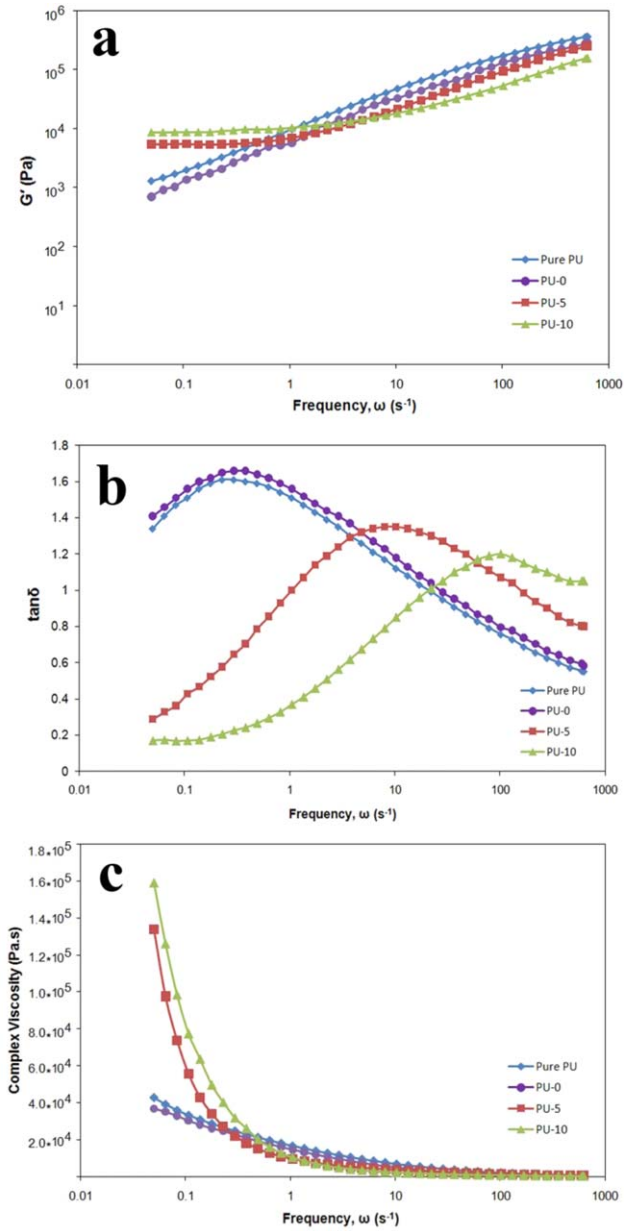

Figure 7. Frequency dependence of (a) G', (b) damping factor, and (c) η^* of pure PU and IFRPU/starch composites performed at 140°C. [Color figure can be viewed in the online issue, which is available at wileyonlinelibrary.com.]

of PU and starch are responsible for enhanced tensile strength. The increment in total heats of fusion (Table IV) can be related to tensile strength. Moreover, addition of the starch into the PU matrix increased the modulus which predicts enhancement of impact toughness. This modulus increment may generally produce a tougher material.[51] As shown in Table V, elongation at break was decreased by starch addition. This decrement could be influenced by several parameters such as degree and shape of crosslinking, the hardness of starch granules, entanglement between amylose and amylopectin, and IFR content.

Morphology of IFRPU/Starch Composites

SEM micrographs of neat starch, unextracted fractured surface of PU-10, and starch extracted of PU-10 (6000× and 800×) are shown in Figure 6(a–d), respectively. The fracture surface of PU-10 was prepared by breaking the samples in liquid nitrogen. Extraction of potato starch was carried out by immersing the fractured specimen in water (25°C) for 3 days. Apart from large void zones induced by starch extraction, there were also some small holes which were not seen in unextracted sample. The appearance of these small holes is due to partial diffusion of water into the bulk of composite under this relatively long time, not because of MCAPP dissolution. It is worthwhile to point out APP solubility in water significantly declines after encapsulation by PU.[52] Strong hydrogen bonding between hard segments of PU and starch is responsible for good dispersion (See section "Thermal Transition of Pure PU and IFRPU/starch composites"). Indeed, these intermolecular attraction forces severely hinder aggregation of IFR system and consequently facilitate dispersion and wetting. Good starch dispersion not only enhances mechanical properties but also improves thermal stability, resulting in the better flame retardancy.

Viscoelasticity Properties of Pure PU and IFRPU/Starch Composites

Viscoelastic or rheological tests are widely used to study composites microstructure and understand the processing conditions during melt state.[53] The frequency dependence of storage modulus also provides a sense of internal dynamics of a polymer blend.[54] Figure 7(a–c) presents the frequency dependence of storage modulus, damping factor, and complex viscosity of pure PU and its composites. As it can be seen, starch containing samples follow solid like behavior ($G_0 \sim \omega$), as expected at $T = 140$°C. In the low frequency region, the IFR and starch incorporation leads to a higher storage modulus (G'), as compared with pure PU and PU-0. The addition of both IFR and starch particles produces a dramatic increase by nearly one and half orders of magnitude at frequencies below 1 Hz. Moreover, the addition of starch to 10 wt % shows the highest G' values among all samples indicating an enhancement in reinforcement [Figure 7(a)]. Starch containing samples exhibit a pronounced nonterminal behavior in storage modulus whose plateau magnitude increases with starch content. The observed nonterminal behavior is an indication of three-dimensional physical network formation induced by interaction of starch with PU which further confirms FTIR results. Indeed, starch establishes a synergism in the dynamical properties corresponding to the formation of internal networks. Chen et al.[33] described a direct linear relation between entangled network formations and improved flame retardant properties, which is essentially originated from improved structure of the char layer. Addition of fillers usually restricts the chain movement and further enhances relaxation time of polymer chains (τ). τ can be obtained from the reciprocal of frequency where G' intersects with G'' (namely, where tan $\delta = 1$) [Figure 7(b)].[55]

The η^* values display a similar trend to those of G' and are significantly increased by adding IFR and starch especially in the low frequency such as 0.01 rad/sec [Figure 7(c)]. From another perspective, melt viscosity increment in starch

containing samples implies the fact that mechanism of flame retardancy is analogous to a condensed-phase phenomenon originated from the formation of a thermal protection or mass loss barrier.[56,57]

CONCLUSION

In our research, starch along with MCAPP and MA were used to develop a PU-based composite with improved flame retardancy. Pure PU was combustible, whereas PU composites containing 20% IFR and 10% starch could reach UL-94 V0 with a high LOI value of 40. Mechanical properties improved due to crosslinking between starch and PU matrix. TGA results indicated that addition of starch into PU dramatically improved char yields and thermal stability at high temperature, as compared with pure PU. Nonterminal behavior further verified three-dimensional physical network structures in these IFRPU/starch composites. A blanket-like char layer mainly composed of carbon/pyrophosphate and/or polyphosphate compounds notably performed as a protective barrier layer and restricted the oxygen diffusion to the surface. FTIR confirmed the presence of hydrogen bonding between starch and PU.

ACKNOWLEDGMENTS

We are immensely grateful to Mr. Jalal Nasrollah Gavgani for supporting us financially and Miss Taleb for her great guidance.

REFERENCES

1. Howard, G. T. *Int. Biodeterior. Biodegrad.* **2002**, *49*, 245.
2. Oprea, S.; Oprea, V. *Eur. Polym. J.* **2002**, *38*, 1205.
3. Feng, Y.; Li, C. *Polym. Degrad. Stab.* **2006**, *91*, 1711.
4. Sarkar, D.; Lopina, S. T. *Polym. Degrad. Stab.* **2007**, *92*, 1994.
5. Bourbigot, S.; Bras, M. L.; Duquesne, S.; Rochery, M. *Macromol. Mater. Eng.* **2004**, *289*, 499.
6. European Commission. *Off. J. Eur. Union* **2003**, *L 37*, 19.
7. Nie, S. B.; Song, L.; Guo, Y. Q.; Wu, K.; Xing, W. Y.; Lu, H. D.; Hu, Y. *Ind. Eng. Chem. Res.* **2009**, *48*, 10751.
8. B. Li, MJ. Xu, *Polym. Degrad. Stab.* **2006**;*91*:1380.
9. Lee, D. H.; Hyun, D. H.; Gwon, S. H.; Cho, H. D.; Kim, S. B. U.S. Pat. 0,236,*132* (**2004**).
10. Andrade, M. M. P.; de Oliveira, C. S.; Colman, T. A. D.; da Costa, F. J.; Schnitzler, E. *J. Therm. Anal. Calorim.* **2014**, *114*, 2115.
11. Fan, F.; Xia, Z.; Li, Q.; Li, Z.; Chen, H. *J. Therm. Anal. Calorim.* **2013**, *114*, 937.
12. Laoutid, F.; Bonnaud, L.; Alexandre, M.; Lopez-Cuesta, J. M.; Dubois, P. *Mater. Sci. Eng. Rep.* **2009**, *63*, 100.
13. Nie, S.; Qi, S.; He, M.; Li, B. *J. Therm. Anal. Calorim.* **2013**, *114*, 581.
14. Jimenez, M.; Duquesne, S.; Bourbigot, S. *Ind. Eng. Chem. Res.* **2006**, *45*, 4500.
15. Ni, J. X.; Song, L.; Hu, Y.; Zhang, P.; Xing, W. Y. *Polym. Adv. Technol.* **2009**, *20*, 999.
16. Ni, J. X.; Chen, L. J.; Zhao, K. M.; Hu, Y.; Song, L. *Polym. Adv. Technol.* **2011**, *22*, 1824.
17. Wu, K.; Wang, Z. Z.; Hu, Y. *Polym. Adv. Technol.* **2008**, *19*, 1118.
18. Li, L.; Qian, Y.; Jiao, C. M. *J. Therm. Anal. Calorim.* **2013**, *114*, 45.
19. Wang, X. C.; Zhang, X. X.; Liu, H. H.; Wang, N. *Starch/Starke* **2009**, *61*, 489.
20. Lu, X. L.; Du, F. G.; Ge, X. C.; Xiao, M.; Meng, Y. Z. *J. Biomed. Mater. Res.* **2006**, *77*, 653.
21. Zhang, J. F.; Sun, X. *Biomacromolecules* **2004**, *5*, 1446.
22. Kweon, D. K.; Kawasaki, N.; Nakayama, A.; Aiba, S. *J. Appl. Polym. Sci.* **2004**, *92*, 1716.
23. Kisku, S. K.; Swain, S. K. *Polym. Compos.* **2012**, *33*, 79.
24. Wu, K.; Hu, Y.; Song, L.; Lu, H. D.; Wang, Z. Z. *Ind. Eng. Chem. Res.* **2009**, *48*, 3150.
25. Potts, J. R.; Murali, S.; Zhu, Y. W.; Zhao, X.; Ruoff, R. S. *Macromoleculses* **2011**, *44*, 6488.
26. Solar, L.; Nohales, A.; Muñoz-Espí, R.; López, D.; Gómez, C. M. *J. Polym. Sci. Part B: Polym. Phys.* **2008**, *46*, 1837.
27. Wang, X.; Song, L.; Yang, H.; Lu, H.; Hu, Y. *Ind. Eng. Chem. Res.* **2011**, *50*, 5376.
28. Ni, J.; Tai, Q.; Lu, H.; Hu, Y.; Song, L. *Polym. Adv. Technol.* **2010**, *21*, 392.
29. Duquesne, S.; Bras, M. L.; Bourbigot, S.; Delobel, R.; Camino, G.; Eling, B.; Lindsay, C.; Roels, T.; Vezin, H. *J. Appl. Polym. Sci.* **2001**, *82*, 3262.
30. Albu, P.; Bolcu, C.; Vlase, G.; Doca, N.; Vlase, T. *J. Therm. Anal. Calorim.* **2011**, *105*, 685.
31. Luda, M. P.; Nada, P.; Costa, L.; Bracco, P.; Levchik, S. V. *Polym. Degrad. Stab.* **2004**, *86*, 33.
32. Ravey, M.; Pearce, E. M. *J. Appl. Polym. Sci.* **1997**, *63*, 47.
33. Chen, M.; Shao, Z. B.; Wang, X. L.; Chen, L.; Wang, Z. L. *Ind. Eng. Chem. Res.* **2012**, *51*, 9769.
34. Likozar, B.; Korošec, R. C.; Poljanšek, I.; Ogorelec, P.; Bukovec, P. *J. Therm. Anal. Calorim.* **2012**, *109*, 1413.
35. Grassie, N.; Mendoza, G. *Polym. Degrad. Stab.* **1985**, *11*, 359.
36. Price, D.; Liu, Y.; Milnes, G. J.; Hull, R.; Kandola, B. K.; Horrocks, A. R. *Fire Mater.* **2002**, *26*, 201.
37. Thirumal, M.; Khastgir, D.; Nando, G. B.; Naik, Y. P.; Singha, N. K. *Polym. Degrad. Stab.* **2010**, *95*, 1138.
38. Ha, S.; Broecker, H. C. *Polymer* **2002**, *43*, 5227.
39. Cao, X.; Zhang, L.; Huang, J.; Yang, G.; Wang, Y. *J. Appl. Polym. Sci.* **2003**, *90*, 3325.
40. Wan, X.; Hu, Y.; Song, L.; Xuan, S.; Xing, W.; Bai, Z.; Lu, H. *Ind. Eng. Chem. Res.* **2011**, *50*, 713.
41. Shanks, R. A.; Wasantha, L. M.; Gunaratne, K. *J. Therm. Anal. Calorim.* **2011**, *106*, 93.
42. Li, Y.; Li, B.; Dai, J.; Jia, H.; Gao, S. *Polym. Degrad. Stab.* **2008**, *93*, 9.
43. Singh, H.; Jain, A. K.; Sharma, T. P. *J. Appl. Polym. Sci.* **2008**, *109*, 2718.
44. Chen, X.; Jiao, C.; Zhang, J. *J. Therm. Anal. Calorim.* **2011**, *104*, 1037.

45. van Ekeren, P. J.; Carton, E. P. *J. Therm. Anal. Calorim.* **2011**, *105*, 591.

46. Hesketh, T. R.; Van Bogart, J. W. C.; Cooper, S. L. *Polym. Eng. Sci.* **1980**, *20*, 190.

47. Seymour, R. W.; Cooper, S. L. *Macromolecules* **1973**, *6*, 48.

48. Wu, Q.; Wu, Z.; Tian, H.; Zhang, Y.; Cai, S. *Ind. Eng. Chem. Res.* **2008**, *47*, 9896.

49. Dai, J. F.; Li, B. *J. Appl. Polym. Sci.* **2010**, *116*, 2157.

50. Isitman, N. A.; Kaynak, C. *Polym. Degrad. Stab.* **2010**, *95*, 1523.

51. Pack, S.; Kashiwagi, T.; Stemp, D.; Koo, J.; Si, M.; Sokolov, J. C.; Rafailovich, M. H. *Macromolecules* **2009**, *42*, 6698.

52. Wang, B.; Hu, S.; Zhao, K.; Lu, H.; Song, L.; Hu, Y. *Ind. Eng. Chem. Res.* **2011**, *50*, 11476.

53. Somomon, M. J.; Almusallam, A. S.; Seefeldt, K. F.; Somwangthanaroj, A.; Varadan, P. *Macromolecules* **2001**, *34*, 1864.

54. Koo, J.; Shin, K.; Seo, Y.; Koga, T.; Park, S.; Satija, S.; Chen, X.; Yoon, K.; Hsiao, B. S.; Sokolov, J. C.; Rafailovich, M. H. *Macromolecules* **2007**, *40*, 9510.

55. Cao, Q.; Song, Y. H.; Tan, Y. Q.; Zheng, Q. *Polymer* **2009**, *50*, 6350.

56. Kashiwagi, T.; Mu, M. F.; Winey, K.; Cipriano, B.; Raghhavan, S. R.; Pack, S.; Rafailovich, M.; Yang, Y.; Grulke, E.; Shields, J.; Harris, R.; Douglas, J. *Polymer* **2008**, *49*, 4358.

57. Ma, H. Y.; Tong, L. F.; Xu, Z. B.; Fang, Z. P. *Adv. Funct. Mater.* **2008**, *18*, 414.